

# Mechanisms of Ignition by Transient Energy Deposition: Regimes of Combustion Waves Propagation

A.D. Kiverin<sup>1,\*</sup>, D.R. Kassoy<sup>2</sup>, M.F. Ivanov<sup>1</sup>, and M.A. Liberman<sup>3,4†</sup>

<sup>1</sup> *Joint Institute for High Temperatures, Russian Academy of Science, Izhorskaya 13, Bld. 2 Moscow 125412, Russia*

<sup>2</sup> *Department of Mechanical Engineering, Box 427,  
University of Colorado, Boulder, Colorado 80309, USA*

<sup>3</sup> *Moscow Institute of Physics and Technology, Dolgoprudnyi, 141700, Russia*

<sup>4</sup> *Nordita, KTH Royal Institute of Technology and Stockholm University, Roslagstullsbacken 23, 10691 Stockholm, Sweden*

(Dated: October 6, 2018)

Regimes of chemical reaction wave propagating in reactive gaseous mixtures, whose chemistry is governed by chain-branching kinetics, are studied depending on the characteristics of a transient thermal energy deposition localized in a finite volume of reactive gas. Different regimes of the reaction wave propagation are initiated depending on the amount of deposited thermal energy, power of the source and the size of the hot spot. The main parameters which define regimes of the combustion waves facilitated by the transient deposition of thermal energy are: acoustic timescale, duration of the energy deposition, ignition time scale and size of the hot spot. The interplay between these parameters specifies the role of gasdynamical processes, the formation and steepness of the temperature gradient and speed of the spontaneous wave. The obtained results show how ignition of one or another regime of combustion wave depends on the value of energy, rate of the energy deposition and size of the hot spot, which is important for the practical use and for risk assessment.

PACS numbers: 47.70.Pq, 82.33.Vx, 47.40.Rs

## I. INTRODUCTION

The initiation or ignition of a chemical reaction is one of the most important and fundamental problems in combustion physics. One needs to know how combustion starts and how the transient energy deposition influences the regime of the reaction wave which propagates out from a finite volume of reactive gas where a transient thermal energy were deposited - the hot spot. What type of combustion wave is formed depending on: the amount of energy actually added to a finite volume of reactive gas on a specific time scale, the power deposition, and the ignition conditions, e.g. size of the hot spot, initial pressure, etc.? Long ago Oppenheim and Soloukhin<sup>1</sup> recognized the importance of these concepts with the remark "Gasdynamics of Explosions is best defined as the science dealing with the interrelationship between energy transfer occurring at a high rate in a compressible medium and the concomitant motion set up in this medium". The community of scholars has sought to address this perspective for many years represented by a vast combustion science literature too extensive to enumerate here.

Transient thermal energy deposition into a reactive gas provides a source for ignition of either deflagration or detonation. Sufficiently fast and large energy addition can facilitate direct initiation of detonation. However the particular mechanism of the direct initiation of detonation can be different. Detonation can be initiated by a strong shock (strong explosion) or it can arise as a result of the formation of an appropriate temperature gradient through the Zeldovich' gradient mechanism<sup>2</sup>. In most practical cases ignition arises from a small volume of combustible mixture which is locally heated by

energy input by means of an electric spark, hot wire, focused laser light and other related external sources. Such a transient energy addition process can generate a wide range of gas expansion processes depending on the amount and the rate of energy actually added and may result in the formation of the initial non-uniform distribution of temperature (see for example, Kassoy<sup>3,4</sup> for the diverse range of fluid responses to localized, spatially distributed, thermal power addition into an inert gas). An example of an initial nonuniform distribution of temperature arises from the energy deposition of a spark-plug in an engine combustor<sup>5</sup>. In the general case it can be non-uniform distributions of temperature, pressure and/or concentration of reactants which determine further evolution of the reaction wave depending on the mixture reactivity and initial pressure. An example of concentration non-uniformity is a hydrogen gas leakage and its nonuniform distribution by convective mixing in a room. In all cases, a reaction wave arises from the induction time non-uniformity via the thermal explosion.

The ignition problem is important for improving combustion safety and risk assessments of processes where hydrocarbons are oxidized at different initial conditions (concentration, temperature and pressure). How can we minimize "accidental" explosions in mines, chemical industry and nuclear power plants? An important problem of "hydrogen safety" is connected with leakage of hydrogen gas, subsequent mixing with air and the mixture explosion due to local heat release. It is worth noting that the problem in question is also of great interest for hydrogen storage, transportation and utilization and for the design and operation of perspective pulse detonation engines and homogeneous charge compression ignition (HCCI) engines.

For the first time possible regimes of chemical reaction wave ignited by the initial non-uniform distribution of temperature have been studied by Ya. B. Zeldovich using a one-step chemical reaction model<sup>2</sup>. The basic idea of the Zeldovich's concept was that a spontaneous reaction wave can propagate through a reactive material along a spatial gradient of temperature  $\nabla\mathbf{T}(\mathbf{x})$ , with the velocity

$$U_{sp} = |(d\tau_{ind}/dx)|^{-1} = \left| (\partial\tau_{ind}/\partial T)^{-1} (\partial T/\partial x)^{-1} \right| \quad (1)$$

where  $\tau_{ind}(T(x))$  is the induction time. The value of  $U_{sp}$  depends only on the steepness of the temperature gradient. Then the regime of the formed combustion wave depends on the value of spontaneous wave velocity compared to the sound speed.

Recently regimes of chemical reaction wave propagation initiated by initial temperature non-uniformity in gaseous mixtures, whose chemistry is governed by chain-branching kinetics, were studied using a multispecies transport and detailed chemical model<sup>6</sup>. Possible regimes of the reaction wave propagation were identified for the stoichiometric hydrogen/oxygen and hydrogen/air mixtures in a wide range of initial pressures and temperature level depending on the initial gradient steepness.

The question that still remained unanswered is how the temperature gradient in the Zeldovich's concept of the spontaneous reaction wave<sup>2</sup> arises. Kassoy and co-authors<sup>7-13</sup> use a one step chemical reaction model to study how a temperature distribution adjacent to a planar boundary, generated either by direct deposition of transient, spatially distributed thermal power into a defined volume of reactive gas, or by conduction through the boundary into the gas, leads to planar detonation initiation. The authors seek to understand the magnitude of the energy addition deposited on specific time and length scales required to produce conditions that will lead to detonation initiation. The important difference between a one-step and detailed chemical models is seen, for example, from the result of<sup>14</sup>, where it was shown the ignition energy for methane-air computed using a one-step model differs by two orders of magnitude from the experimentally measured value.

Liberman et. al<sup>6</sup> take a different approach to show that steepness of an imposed temperature gradient (the length scale at fixed temperature difference) required for initiating combustion regimes, in particular a detonation, in gaseous mixtures with chain-branching kinetics, may differ up to several orders of magnitude from that obtained using a one step global chemical reaction model. The energy of ignition for hydrogen-oxygen gaseous mixture has been calculated in<sup>15</sup> using a detailed reaction mechanism and a multispecies transport model, but difference in ignition of different combustion regimes remained unanswered.

The purpose of the present paper is to study how the initial temperature gradient is formed depending on the rate and amount of energy addition, on the size of hot spot and on the gasdynamic processes emerging in the region of transient energy deposition. The problem of

great practical importance is: how is temperature non-uniformity initiating different combustion regimes arise? How do the gasdynamic processes caused by the energy addition influence the formation of the temperature gradient and how it depends on the rate and amount of energy input and on the size of hot spot? Solution of this problem answers the question of great practical importance: what is the amount of energy and how it should be deposited to ignite certain regimes of combustion wave. The paper presents new results on classification of the propagation regimes of chemical reaction wave initiated by the transient energy deposition in gaseous mixtures using high resolution numerical simulations of reactive Navier-Stokes equations, including a multispecies transport model, the effects of viscosity, thermal conduction, molecular diffusion and a detailed chemical reaction mechanism for hydrogen-oxygen mixture which is the quintessential example of chain branching reactions whose chemical kinetics is well understood and whose detailed chemical kinetic models are well known and relatively simple. Such a level of modeling allows clear understanding of the feedback between gasdynamics and chemistry, the principal point when studying unsteady process of ignition, not easily be captured using simplified gas-dynamical and chemical models.

High fidelity reliable numerical simulations of the present study are performed to identify ignition processes in homogeneous hydrogen-oxygen mixtures caused by the localized energy deposition. The distinct ignition regimes are identified depending on the size of the hot spot, energy amount, the duration of energy addition and initial pressure. The obtained results open perspectives for understanding of how to avoid or on the contrary what are the conditions to initiate different combustion regimes (slow deflagration, fast deflagration, detonation). The performed analysis reveals the conditions when detonation is initiated as a result of direct initiation by a strong shock wave, or when it results from the formation of suitable temperature gradient for the Zeldovich's mechanism of detonation triggering. The amount and the rate of energy addition needed to form a proper gasdynamics nonuniformity for triggering either detonation or deflagration waves are found.

## II. PROBLEM SETUP

We consider uniform initial conditions and a transient external source of energy localized on the scale of the "hot spot"  $0 \leq x \leq L$ , where energy  $Q_{ig}$  is added during the time  $\Delta t_Q$ . Gasdynamics of the explosion initiated by the localized energy deposition is characterized by the interrelationship between the rate of energy transfer with the time characterizing energy deposition  $\Delta t_Q$  in the hot spot of size  $L$  and the characteristic times of the problem. For the sake of simplicity we assume that the rate of the energy addition is constant in time, so that total energy deposition into the hot spot is  $Q_{ig} = W\Delta t_Q$ , where  $W$

is the power of the external source of energy, and  $\Delta t_Q$  is time of the hot spot transient heating. The characteristic acoustic time  $t_a = L/a(T)$  defines the concomitant motion setup in the gaseous mixture, where  $a(T)$  is the speed of sound. If  $\Delta t_Q \ll t_a$  local heat addition occurs as a nearly constant volume process and the temperature elevation within the hot spot is accompanied by a concomitant pressure rise. Subsequent expansion of the hot spot driven by the large pressure gradient between the hot spot and the ambient gas causes compression and shock waves in the surrounding ambient gas. When  $\Delta t_Q \gg t_a$  the acoustic waves have enough time for pressure equalization and the local heat addition occurs at nearly constant pressure.

The local heat of gaseous mixture within the hot spot leads to the heat being concentrated in a small region from which heat propagates into the surrounding gas according to well known solution of the equation of thermal conduction<sup>16</sup>. For the one-dimensional case the temperature distribution (for constant thermal diffusivity) is

$$T(x, t) \propto \frac{1}{2\sqrt{\pi\chi t}} \exp(-x^2/4\chi t) \quad (2)$$

where  $\chi = \kappa(T)/\rho C_P$  is the coefficient of thermal diffusivity. It follows from Eq. (2) that heat propagates at the distance  $x \sim \sqrt{4\chi t}$  and temperature in the surrounding gas increases noticeably due to propagation of a thermal wave during the time

$$t_T \sim x^2/\chi \quad (3)$$

At the very beginning the thermal wave propagates with the velocity  $dx/dt \sim \sqrt{\chi/t}$  overtaking the shock wave, which propagates with a velocity approximately equal to the sound speed in the heated gas.

However, very soon the shock wave overtakes the thermal wave, so that characteristic thermal wave time is effectively much longer than the acoustic time. For example,  $t_T \sim x^2/\chi \approx 0.1s$  and  $t_a \sim 2\mu s$  for  $x \simeq 1mm$  for hydrogen-oxygen mixture at  $P = 1atm$ .

Whether a chemical reaction starts and which processes define the regime of combustion wave depend on the interrelationship between  $\Delta t_Q$ ,  $t_a$ ,  $t_T$  and induction time  $t_{ind}(T)$  at the existing temperature and pressure. The induction time is the time scale for the stage of endothermic chain initiation and branching reactions (in the case of a global one-step reaction this is the time-scale for the maximum reaction rate). Here it is suitable to use the scale of ignition time  $t_{ign}$ , characterizing the length of induction phase after or during the transient energy deposition  $t_{ind}(T, P)$ . The induction time is measured experimentally and determines local properties of the combustible mixture depending on its thermodynamic state. Dependence of the induction time on temperature for a hydrogen-oxygen mixture at initial pressures  $P_0 = 1atm$  and  $P_0 = 10atm$  is shown in Fig. 1.

For the temperature range  $T = (1100 - 1500)K$ , where the exothermic reaction starts, the induction time is

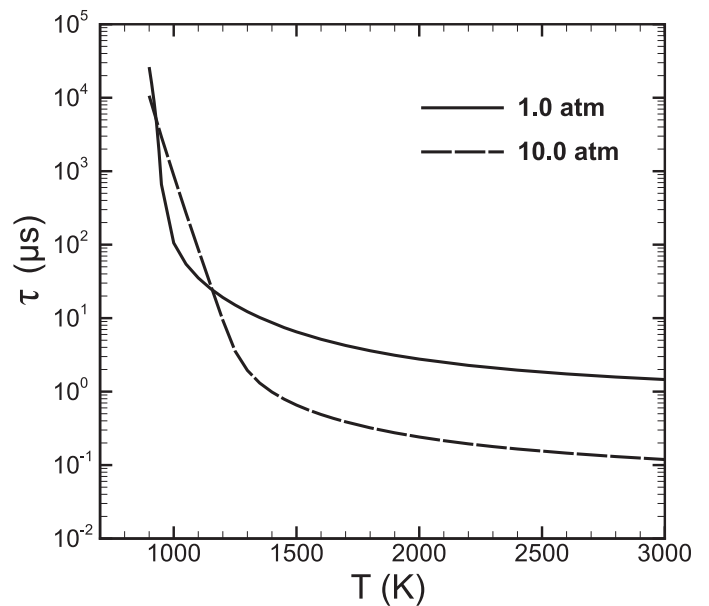


FIG. 1. Induction time for hydrogen-oxygen stoichiometric mixture at different temperatures and pressures:  $P_0 = 1atm$  (solid line) and  $P_0 = 10atm$  (dashed line).

about ten microseconds. If the reaction has started, further heating and energy deposition do not matter and do not influence the formed combustion regime. Thus, primary interest is focused on the regimes of ignition with  $\Delta t_Q < t_{ign}$ . For a very short time of energy addition, much less than the acoustic time, the mixture in the hot spot can be heated to any temperature and the ignition regime will be determined by the induction time at that temperature and accompanying pressure. In case of a more extended energy deposition, the ignition regime will depend on the size of the hot spot (and correspondingly on  $t_a$ ) and the relation between  $\Delta t_Q$  and  $t_a$  as mentioned earlier in reference to the features of the hot spot expansion process.

For a one-dimensional formulation the hot spot represents a region  $0 \leq x \leq L$ , where energy is deposited with the rate  $W(t) = dQ(t)/dt$ . The specific internal energy of the mixture is changed as  $Q(t) = Q(t - \Delta t) + \Delta Q$  within the hot spot during time interval  $\Delta t$ . Total energy at the end of the energy addition depends on the gas-dynamic motion

$$Q_{total} = \sum_{t=0}^{\Delta t_Q} \sum_{x=0}^L \Delta Q \cdot \rho(x, t) \cdot \Delta x. \quad (4)$$

Total energy transfer till the formation of a 1-D stationary combustion wave far from the hot spot (at  $x \gg L$ ) can be viewed as the ignition energy required for initiation of the particular combustion regime.

The governing equations are the one-dimensional time-dependent, multispecies reactive Navier-Stokes equations

including the effects of compressibility, molecular diffusion, thermal conduction, viscosity and chemical kinetics with subsequent chain branching, production of radicals and energy release.

$$\frac{\partial \rho}{\partial t} + \frac{\partial (\rho u)}{\partial x} = 0, \quad (5)$$

$$\frac{\partial Y_i}{\partial t} + u \frac{\partial Y_i}{\partial x} = \frac{1}{\rho} \frac{\partial}{\partial x} \left( \rho D_i \frac{\partial Y_i}{\partial x} \right) + \left( \frac{\partial Y_i}{\partial t} \right)_{ch}, \quad (6)$$

$$\rho \left( \frac{\partial u}{\partial t} + u \frac{\partial u}{\partial x} \right) = - \frac{\partial P}{\partial x} + \frac{\partial \sigma_{xx}}{\partial x}, \quad (7)$$

$$\begin{aligned} \rho \left( \frac{\partial E}{\partial t} + u \frac{\partial E}{\partial x} \right) &= - \frac{\partial (Pu)}{\partial x} + \\ &+ \frac{\partial}{\partial x} (\sigma_{xx} u) + \frac{\partial}{\partial x} \left( \kappa(T) \frac{\partial T}{\partial x} \right) + \\ &+ \sum_k \frac{h_k}{m_k} \left( \frac{\partial}{\partial x} \left( \rho D_k(T) \frac{\partial Y_k}{\partial x} \right) \right) + W(t), \end{aligned} \quad (8)$$

$$P = R_B T n = \left( \sum_i \frac{R_B}{m_i} Y_i \right) \rho T = \rho T \sum_i R_i Y_i, \quad (9)$$

$$\varepsilon = c_v T + \sum_k \frac{h_k \rho_k}{\rho} = c_v T + \sum_k h_k Y_k, \quad (10)$$

$$\sigma_{xx} = \frac{4}{3} \mu \left( \frac{\partial u}{\partial x} \right) \quad (11)$$

The initial conditions at  $t = 0$  are constant pressure and zero velocity of the unburned mixture. At the left boundary at  $x = 0$  the conditions are for a solid reflecting wall, where  $u(0, t) = 0$  and the initial temperature  $T(t = 0) = T_0$ .

Here we use the standard notations:  $P$ ,  $\rho$ ,  $u$ , are pressure, mass density, and flow velocity,  $Y_i = \rho_i/\rho$  - the mass fractions of the species,  $E = \varepsilon + u^2/2$  - the total energy density,  $\varepsilon$  - the internal energy density,  $R_B$  - is the universal gas constant,  $m_i$  - the molar mass of i-species,  $R_i = R_B/m_i$ ,  $n$  - the molar density,  $\sigma_{ij}$  - the viscous stress tensor,  $c_v = \sum_i c_{vi} Y_i$  - is the constant volume specific heat,  $c_{vi}$  - the constant volume specific heat of i-species,  $h_i$  - the enthalpy of formation of i-species,  $\kappa(T)$  and  $\mu(T)$  are the coefficients of thermal conductivity and viscosity,  $D_i(T)$  - is the diffusion coefficients of i-species,  $(\partial Y_i/\partial t)_{ch}$  - is the variation of i-species concentration (mass fraction) in chemical reactions.

The equations of state for the reactive mixture and for the combustion products were taken with the temperature dependence of the specific heats and enthalpies of each species borrowed from the JANAF tables and interpolated by the fifth-order polynomials<sup>17,18</sup>. The viscosity and thermal conductivity coefficients of the mixture were calculated from the gas kinetic theory using the

Lennard-Jones potential<sup>19</sup> Coefficient of the heat conduction  $\kappa = \mu C_P / Pr$  for the mixture as a whole is expressed via the viscosity  $\mu$  and the Prandtl number,  $Pr = 0.75$ .

The numerical method is based on splitting of the Eulerian and Lagrangian stages, known as coarse particle method (CPM)<sup>20</sup>. A detailed description of the modified CPM optimal approximation scheme, details of the equations and transport coefficients and the reaction kinetics scheme together with the reaction rates appear in<sup>21,22</sup>. The numerical method is thoroughly tested and successfully used in many practical applications<sup>22-24</sup>.

The convergence of the solutions is of paramount importance to verify that the observed phenomena are sufficiently well resolved, especially when CFD simulations are used with a detailed chemical reaction model. The convergence and resolution tests have shown that the resolution of 50 computational grid cells over the width of a laminar flame (for example, with the grid cell size  $\Delta = 0.0064\text{mm}$  at  $P_0 = 1\text{atm}$ , when the width of a laminar front is  $0.24\text{mm}$ , and much smaller for higher pressure) provides sufficiently good convergence and correctly captures the details of the observed processes (see Appendix in Ref.<sup>6</sup>).

### III. COMBUSTION REGIMES: RAPID ENERGY DEPOSITION - MICROSECOND TIME SCALE

We consider combustion regimes initiated by energy deposition at the initial pressure and temperature  $P_0 = 1\text{atm}$  and  $T_0 = 300\text{K}$  in a hydrogen-oxygen stoichiometric mixture. First we consider cases when the time scale of the energy deposition is comparable to or shorter than the acoustic time scale and less than the induction time at the ignition temperatures. The acoustic time is  $t_a \approx 20\mu\text{s}$  for the hot spot of size  $L = 1\text{cm}$ , and  $t_a \approx 2\mu\text{s}$  for  $L = 1\text{mm}$  ( $a_0(T = 300\text{K}) = 539\text{m/s}$ ). Rapid energy addition into the hot spot on time scales much shorter than acoustic time causes almost uniformly fast elevation of pressure and temperature resulting in the volume explosion. Figure 2 shows the calculated temporal evolution of temperature at the center of the hot spot ( $x = 0$ ) for different values of the transmitted energy, when the energy addition time is very short:  $\Delta t_Q$   $0.1\mu\text{s} < t_{ign} \ll t_a$ . Temperature and pressure of the mixture in the hot spot depend on the energy transmitted to the hot spot. After the end of the energy deposition process, the induction period reaction starts. After about  $10\mu\text{s}$  the stationary combustion regimes are established (see Fig. 2). It should be noted that for each value of deposited energy there is some definite temperature and pressure at which the reaction starts and the combustion regime is produced by the volumetric explosion at these conditions.

For a less rapid process of energy deposition ( $\Delta t_Q = 5\mu\text{s} < t_{ign} < t_a$ ), a large pressure jump is formed at the boundary of the hot spot. If the power is large enough, subsequent events represent the decay of the initial discontinuity consisting of a compression wave propagating

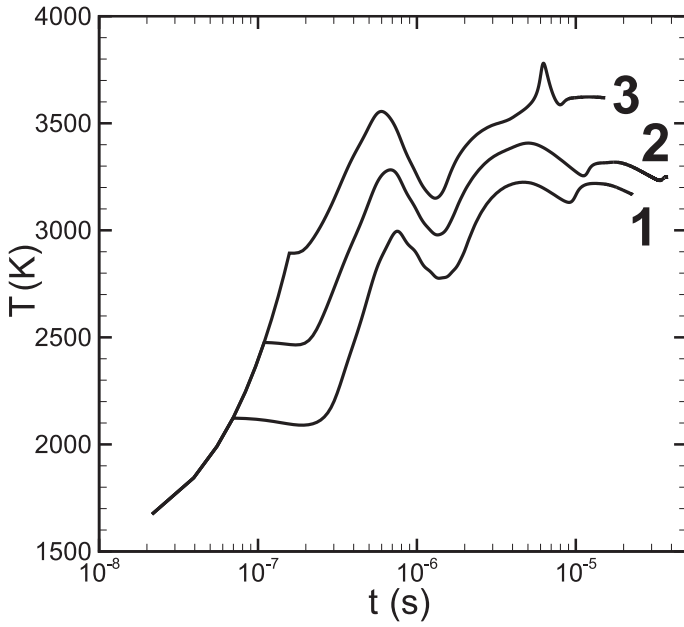


FIG. 2. Temperature evolution in the center of the hot spot for rapid submicrosecond energy deposition  $\Delta t_Q = (0.1 \div 0.2)\mu\text{s}$ ; 1 - deflagration ( $Q = 1.9\text{kJ}/\text{m}^2$ ), 2 - deflagration ( $Q = 2.4\text{kJ}/\text{m}^2$ ), 3 - detonation ( $Q = 3.0\text{kJ}/\text{m}^2$ ).

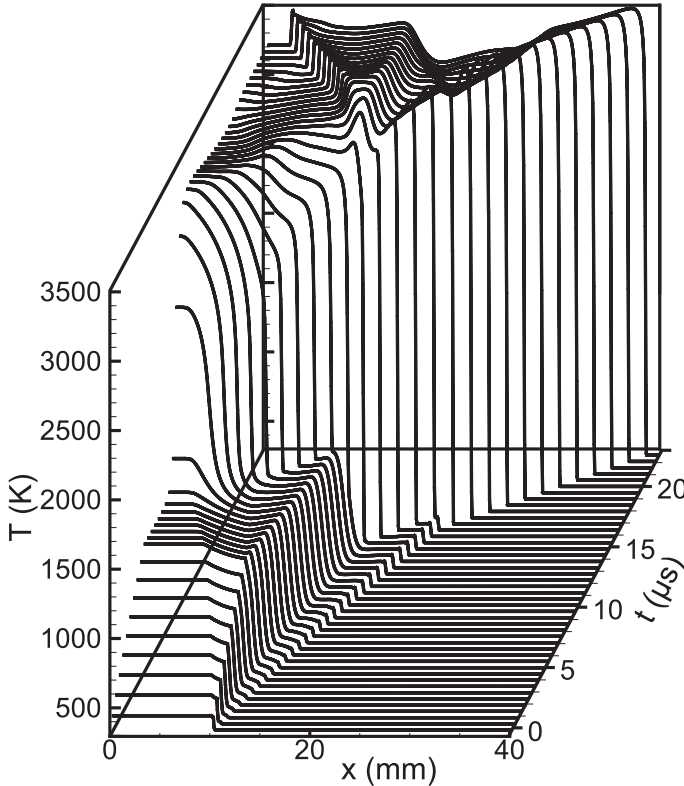


FIG. 3. Evolution of temperature profiles illustrating detonation formation in the energy release region.  $L = 1\text{cm}$ ,  $\Delta t_Q = 5\mu\text{s}$ . Profiles are presented for time instants with interval  $\Delta t_Q = 0.5\mu\text{s}$ .

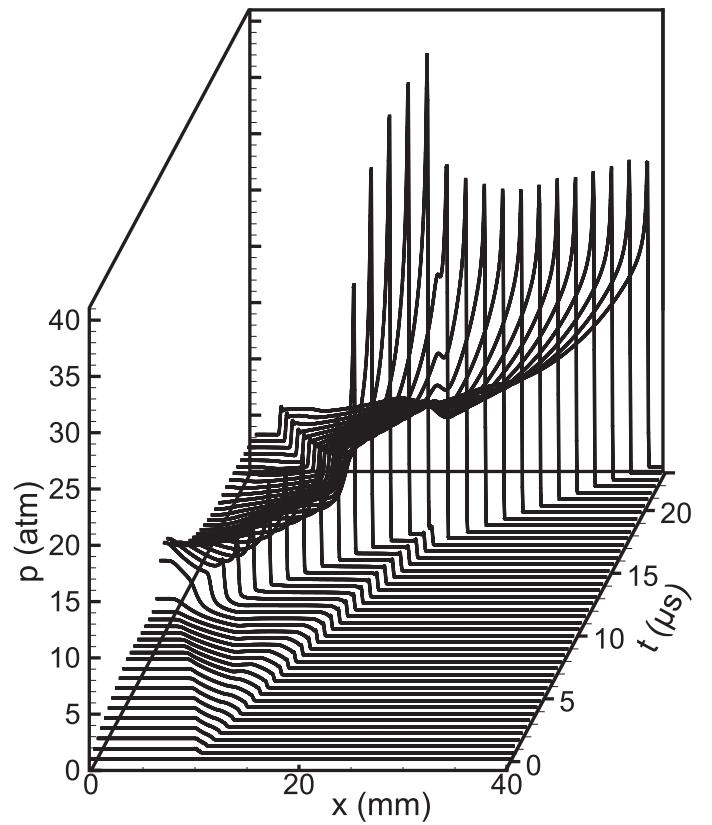


FIG. 4. Evolution of pressure profiles illustrating detonation formation in the energy release region.  $L = 1\text{cm}$ ,  $\Delta t_Q = 5\mu\text{s}$ . Profiles are presented for time instants with interval  $\Delta t_Q = 0.5\mu\text{s}$ .

in the direction  $x > 0$ , which steepens into the shock wave and the rarefaction wave propagating to the left from the boundary of hot spot (in the direction  $x = 0$ ) with the velocity equal to the local sound speed. Such a scenario, which is similar to a strong point explosion<sup>25,26</sup> results in the direct triggering of a detonation wave if a concomitant shock wave at the right boundary is strong enough. A more interesting scenario emerges in the case of a weaker shock and is shown in Fig. 3 and Fig. 4. These figures show the calculated transient evolution of the temperature (Fig. 3) and pressure (Fig. 4) profiles inside the hot spot ( $L = 1\text{cm}$ ) during the energy deposition. The rarefaction wave propagating to the left creates shallow temperature and pressure gradients on the scale of about the size of the hot spot. At an initial pressure of  $P_0 = 1\text{atm}$  the temperature gradient with the temperature difference and length scale  $L \sim 1\text{cm}$  as in Figs. 3, 4 cannot trigger detonation. However, since the pressure of the heated mixture increased during the heating up to  $P \approx 4\text{atm}$ , this temperature gradient can produce a detonation through the Zeldovich gradient mechanism. Time evolution of the temperature and pressure profiles shown in Figs. 3, 4 demonstrate also the emergence of the spontaneous reaction wave and its coupling with the pressure

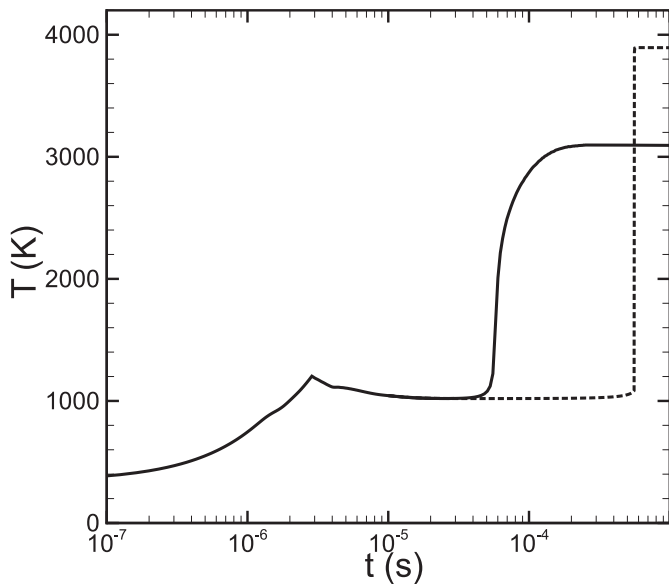


FIG. 5. Temperature evolution in the center of the hot spot for case of low energy deposition ( $t_a < \Delta t_Q < t_{ind}$ ).  $L = 1\text{mm}$ ,  $\Delta t_Q = 16\mu\text{s}$  (solid line),  $P_0 = 10\text{atm}$  (dashed line).

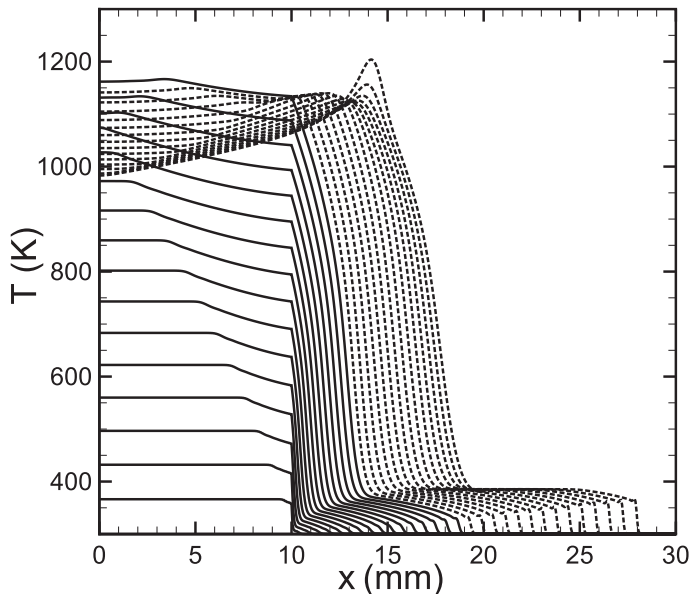


FIG. 6. Evolution of temperature profiles in the hot spot during energy deposition (solid lines) and during induction phase (dashed lines).  $L = 1\text{cm}$ ,  $\Delta t_Q = 16\mu\text{s}$ . Profiles are presented for time instants with interval  $\Delta t = 1\mu\text{s}$ .

wave leading to the detonation initiation through the Zeldovich mechanism.

In case when the ignition time is greater than acoustic time and the energy addition time is less than acoustic time  $\Delta t_Q < t_a < t_{ign}$  the gradient induced by the rarefaction wave forms on the stage after the end of energy addition. During the relatively long induction phase the acoustic perturbations equalize pressure in the en-

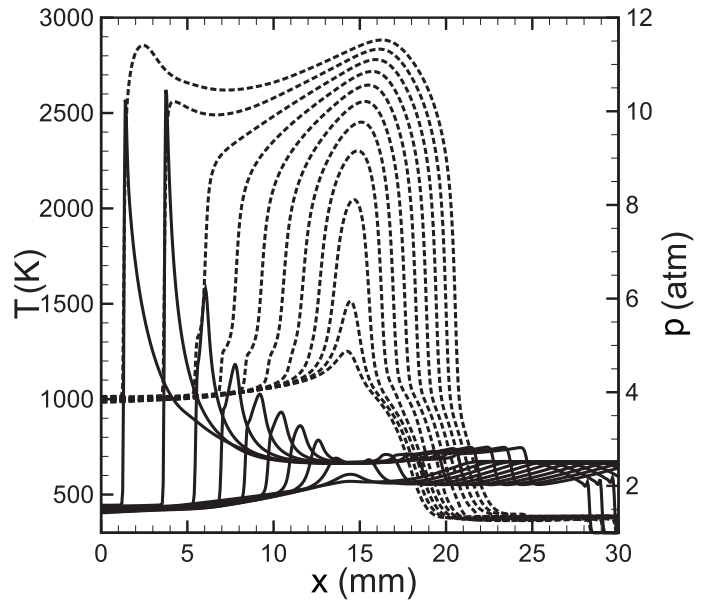


FIG. 7. Evolution of temperature (dashed lines) and pressure (solid lines) profiles illustrating ignition process in the energy release region,  $L = 1\text{cm}$ ,  $\Delta t_Q = 16\mu\text{s}$ . Profiles are presented for time instants with interval  $\Delta t = 1\mu\text{s}$ .

ergy deposition zone and further ignition processes evolve at constant pressure from the steady temperature gradient. Temperature in the top of gradient remains nearly constant till the ignition takes place (see Fig. 5). The combustion regime forming in this case depends on the environmental conditions (e.g. pressure<sup>6</sup>): at  $P_0 = 1\text{atm}$  such a temperature gradient causes deflagration wave formation, at  $P_0 = 10\text{atm}$  it causes detonation wave.

An interesting scenario takes place when the energy deposition time is slightly longer than acoustic time,  $\Delta t_Q = 20\mu\text{s}$ , so that  $t_a < \Delta t_Q < t_{ign}$ . At the beginning the gasdynamics process is similar to the previous case. However, the heating time is longer, and the rarefaction wave has time to reach the left wall, to be reflected from the wall and return to the edge of the hot spot during time of the energy deposition (15 in Ref. <sup>16</sup>). As a result even before the reaction started the hot spot expands with the temperature profile in the mixture consisting of a shallow temperature gradient in the direction to  $x > 0$  and a steep temperature gradient in the direction  $X = 0$ . The initial stage of the temperature time evolution, before the reaction has started, is depicted in Fig. 6. By the time the reactions begins at the top of the gradients, the right side gradient is too steep to trigger a detonation. Instead a deflagration wave propagating to the right is ignited (Ref. <sup>6</sup>). At the same time due to the elevated pressure the left shallow gradient can facilitate triggering detonation through the Zeldovich gradient mechanism. The corresponding time evolution of temperature and pressure profiles showing propagation of the spontaneous wave to the left along the temperature gradient, its coupling with the pressure waves and detonation initia-



tion as well as deflagration initiation by the right steep temperature gradient are depicted in Fig. 7.

The rapid energy deposition such that the heating time,  $\Delta t_Q$ , is comparable to the characteristic acoustic time scale of the volume,  $t_a$ , always results in the shock waves propagating away from the hot spot. A particular scenario of the resulting combustion regime depends on the size of the hot spot, though the basic physics appears to be similar to that described above. In the case of the smaller size of the hot spot ( $L = 1\text{mm}$ ) scenario of the combustion regime ignition may differ because the scale of the temperature gradient created by the rarefaction wave may not be compatible with the detonation formation in real mixtures. There are many different scenarios that include direct detonation formation by a strong enough shock wave in the context of a thermal explosion, or the shock waves propagating away from the hot spot producing ignition of the fast deflagration propagating behind the shock waves (regime 3 according to the classification in Ref.<sup>6</sup>).

#### IV. COMBUSTION REGIMES: MILLISECOND TIME SCALE OF ENERGY DEPOSITION

Sufficiently rapid and large amount of thermal energy deposition into a reactive gas can trigger either direct initiation of detonation through a constant volume explosion, or through the Zeldovich gradient mechanism due to the shallow gradient formed by the rarefaction wave at the increased pressures in the hot spot region. In case of the rapid but relatively small energy deposition the resulting regime is a fast deflagration wave Ref.<sup>6</sup>. The scenario for low power thermal energy addition over a longer period of time is different. If the acoustic time is much less than the energy deposition time,  $t_a \ll \Delta t_Q \leq t_{ign}$ , then there is enough time for pressure to be spatially homogenized by acoustic waves. In this case there are no strong compression waves emitted from the hot spot, and the combustion regimes initiated by the energy deposition into the hot spot depend essentially on the steepness of the temperature gradient, which is formed by the thermal wave and gas expansion in the vicinity of the hot spot.

During the time of energy deposition  $\Delta t_Q$  the thermal wave propagates away from the hot spot at the distance  $x_T/mm = (\chi\Delta t_Q)^{1/2} \approx 0.9(\Delta t_Q/ms)^{1/2}$ . Some of the mass in the volume of the hot spot heated by the added energy, therefore of higher temperature, flows away as the temperature increases and the density falls. The expelled mass together with the thermal wave give rise to the temperature gradient in the surrounding mixture behind the boundary of the hot spot. The temperature profile is almost linear because of the weak temperature dependence of the coefficient of thermal conduction ( $\kappa \propto T^{0.75}$ ). Fig. 8a shows the temperature gradient formed at the end of the energy deposition for  $\Delta t_Q = 1000\mu\text{s}$ ,  $L = 1\text{mm}$  (solid lines). A greater distance compared to that created

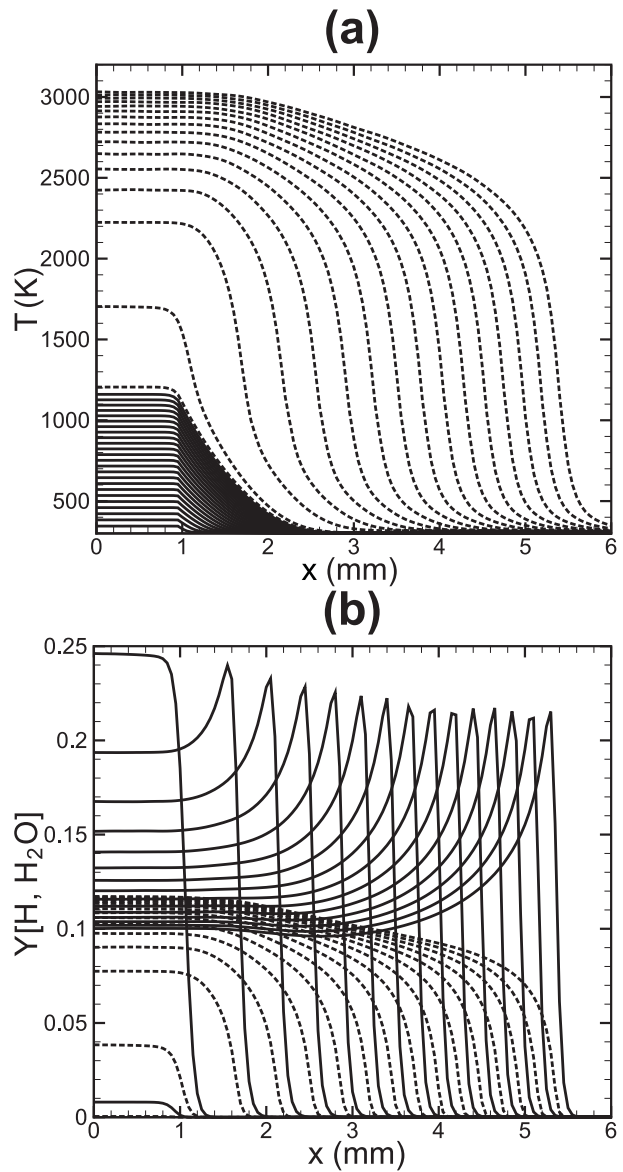


FIG. 8. (a) Evolution of temperature profiles in the hot spot during energy deposition (solid lines) and after it during the combustion wave formation (dashed lines). (b) Evolution of  $H_2O$  concentration (dashed lines) and  $H$ -radical concentration (solid lines) profiles illustrating combustion wave formation on the gradient formed in the energy release region.  $L = 1\text{mm}$ ,  $\Delta t_Q = 1000\mu\text{s}$ . Profiles are presented for time instants with interval  $\Delta t = 5\mu\text{s}$ .

by the thermal wave alone is due to the hot spot expansion, the decreased density and increased temperature in the hot spot during the process of energy deposition. However, according to Ref.<sup>6</sup> this type of linear temperature gradient is too steep to initiate detonation through the Zeldovich gradient mechanism and as a result a deflagration wave is initiated. The thermal wave and the gas expansion are too slow to expand temperature and to form a temperature gradient compatible with the detonation formation in real mixtures at atmospheric or lower

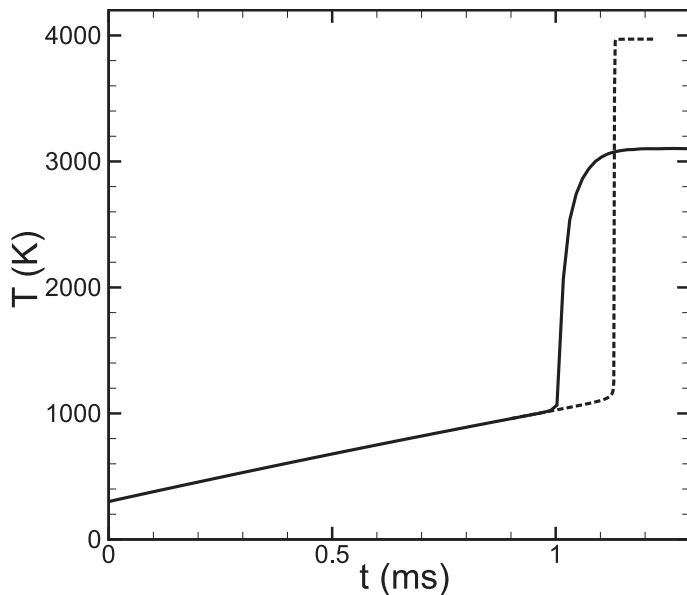


FIG. 9. Temperature evolution in the center of the hot spot for case of slow energy deposition ( $t_a \ll \Delta t_Q$ ).  $L = 1\text{mm}$ ,  $P_0 = 1\text{atm}$  (solid line),  $P_0 = 10\text{atm}$  (dashed line).  $\Delta t_Q = 1000\mu\text{s}$  for  $P_0 = 1\text{atm}$  and  $1100\mu\text{s}$  for  $P_0 = 10\text{atm}$ .

pressures Ref.<sup>6</sup>. Long before the thermal wave moves away a sufficiently long distance the temperature of the mixture rises to ignite the reaction, so that either a deflagration wave or a fast deflagration wave are initiated according to the classification of Ref.<sup>6</sup>. In Fig. 8a dashed lines show the deflagration wave formation out from the formed temperature gradient. Fig. 8b represents the evolution of  $H$ -radical and  $H_2O$  concentration profiles while the combustion wave is forming.

While speed of sound does not depend on pressure, the induction time  $t_{ind}(T)$  at the temperature range (1100 ÷ 1200)K is considerably longer at larger pressures (see Fig. 1). This leads to a significant delay of ignition for the same energy deposition regime at higher pressure. As an example, the growth of temperature at the center of the hot spot  $L = 1\text{mm}$  and at instants when the reaction starts are shown in Fig. 9 for initial pressures  $P_0 = 1\text{atm}$  and  $P_0 = 10\text{atm}$  and for  $\Delta t_Q = 1\text{ms}$ .

Since the coefficient of thermal conductivity does not depend on pressure, and the steepness of the temperature gradient for direct detonation initiation through the Zeldovich gradient mechanism decreases considerably with the increase in pressure Ref.<sup>6</sup>, the temperature gradient created by the thermal wave can trigger detonation at high enough initial pressure. To elucidate the process we consider a relatively small hot spot of size,  $L = 1\text{mm}$  at initial pressure  $P_0 = 10\text{atm}$ . For a sufficiently long energy deposition time, the thermal wave creates gradient appropriate for the detonation initiation through the Zeldovich mechanism at  $P_0 = 10\text{atm}$  Ref.<sup>6</sup> (dashed line in Fig. 9). Figure 10a shows the calculated temporal

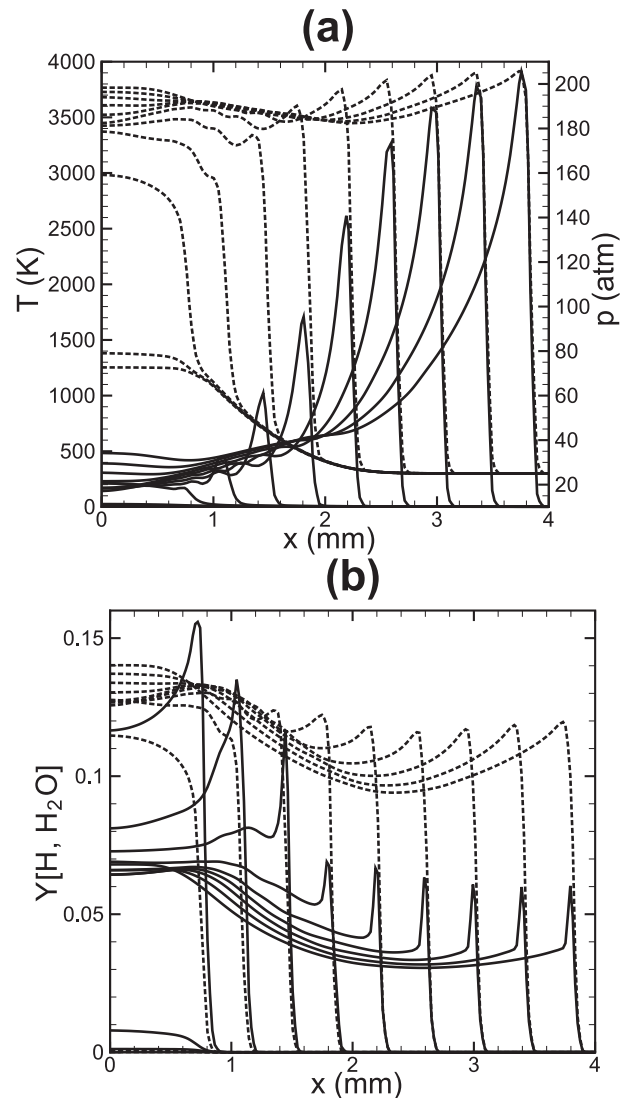


FIG. 10. (a) Evolution of temperature (dashed lines) and pressure (solid lines) profiles illustrating detonation formation on the gradient formed in the energy release region. (b) Evolution of  $H_2O$  concentration (dashed lines) and  $H$ -radical concentration (solid lines) profiles illustrating detonation formation on the gradient formed in the energy release region.  $L = 1\text{mm}$ ,  $\Delta t_Q = 1100\mu\text{s}$ ,  $P_0 = 10\text{atm}$ . Profiles are presented for time instants with interval  $\Delta t = 2\mu\text{s}$ .

evolution of temperature and pressure profiles illustrating formation of the temperature gradient outside of the hot spot,  $L = 1\text{mm}$ , the development of the spontaneous wave along the gradient and transition to detonation for the energy deposition time  $\Delta t_Q = 1\text{ms}$ . Fig. 10b shows the corresponding evolution of the concentration profiles for  $H$ -radicals and the combustion products ( $H_2O$ ).



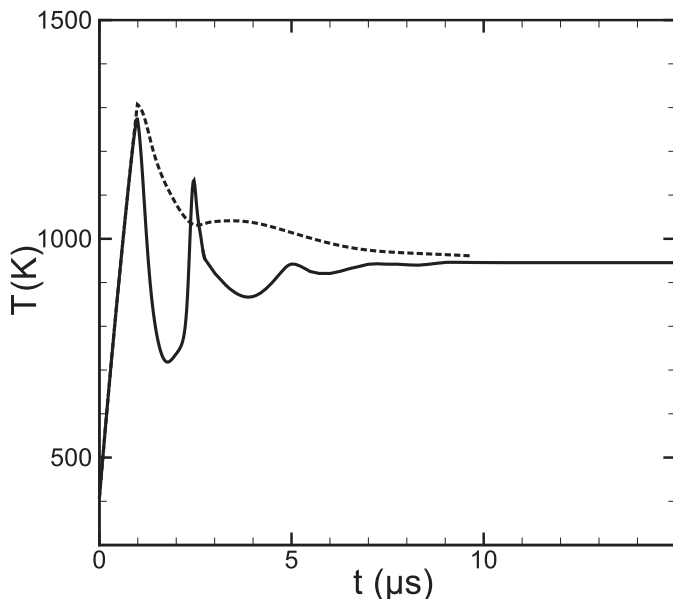


FIG. 11. Temperature evolution in the center of the hot spot for case of rapid energy deposition ( $t_a > \Delta t_Q$ ) in one-dimensional case (dashed line) and three-dimensional case (solid line),  $L = 1\text{mm}$ .

## V. ENERGY OF IGNITION

The results obtained clearly allow us to estimate the energy required for ignition of a particular combustion regime. At the same time it should be noted that the amount of the ignition energy obtained by extrapolating results of the one-dimensional problem most likely will not match the actual value of the ignition energy for the three-dimensional problem where the process is associated with a three-dimensional expansion and converging rarefaction wave. This difference is particularly important for the initiation of detonation. In this case the three dimensional expansion additionally enhances the rarefaction, leading to less suitable conditions for a detonation initiation. A large number of 3D simulations of ignition due to the energy addition to the spherical hot-spot were used to verify realization of different combustion regimes, and to compare the ignition energy obtained from 3D spherically symmetric model to that extrapolated using the 1D model and to assess effect of spherical expansion on the ignition process.

Figure 11 shows the temperature evolution in the center of the hot spot for rapid energy deposition ( $t_a \sim \Delta t_Q$ ) in a one-dimensional case where  $L = 1\text{mm}$  and in the three-dimensional spherical hot spot of radius  $R = 1\text{mm}$ . In both cases the final temperature in the center of the hot spot tends to the same value. Temperature oscillations in the spherical hot spot are caused by convergence of the rarefaction wave to the center and reflection, which is enhanced by the expansion of the gaseous spherical hot spot, where the density decreases approxi-

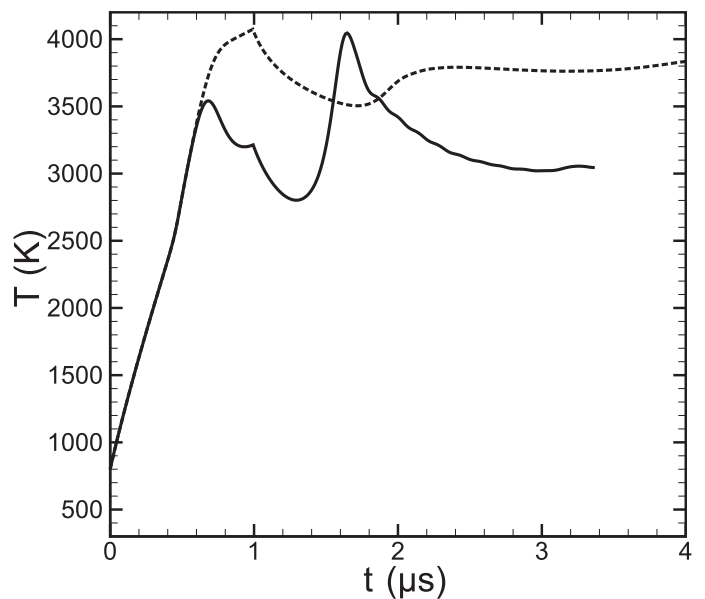


FIG. 12. Temperature evolution in the center of the hot spot for case of rapid energy deposition ( $t_a > \Delta t_Q$ ) in one-dimensional case (dashed line) and three-dimensional case (solid line);  $L = 1\text{mm}$ .

mately as  $\rho \propto \left(1 - (r/R)^2\right)^{\frac{1}{\gamma-1}}$ . Since the rarefaction is much stronger for the 3D spherical expansion, the final temperature of the spherical target is considerably lower than in the planar case at the same parameters of energy deposition if the rarefaction reflects before the energy is deposited ( $t_a < \Delta t_Q$ ). For the same reason, the actual energy required to initiate a detonation is larger for the spherical target than that in the planar case. Even if the temperature of the hot spot rises high enough for initiating detonation in the planar case, it is reduced by the converging and reflecting rarefaction wave and detonation can not be ignited. An example of such a scenario is shown in Fig. 12, where for the same conditions the detonation is initiated in the plane geometry and it is not for a spherical target.

The larger the acoustic time  $t_a$  compared to the time of energy deposition the less the influence of the rarefaction wave on the detonation initiation. This means, for example, that with the increase of the hot spot size (note, that  $t_a \propto L$ ) the initiation of detonation requires less energy deposition into the specific volume of the hot spot for a given time of power deposition  $\Delta t_Q$ , although the total deposited energy will be larger than in the case of detonation initiation in a smaller hot spot using a higher level of power deposition. This tendency is illustrated in Fig. 13. For a shorter period of power deposition the energy amount per unit of volume capable for detonation initiation decreases. The lower limit for hydrogen detonation initiation can be obtained using a short sub-microsecond laser pulse focused in a sub-millimeter area (see e.g. Ref.<sup>27</sup>) and it is estimated as  $\sim 10^{-2}\text{mJ}$ , which

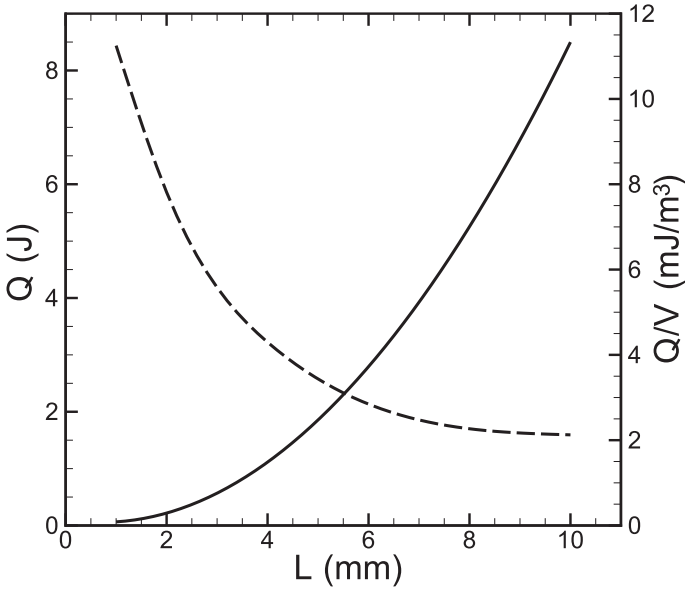


FIG. 13. The minimal energy required for detonation initiation in  $H_2-O_2$  depending on the size (radius) of the hot spot for  $\Delta t_Q = 1\mu s$ . Solid line is total deposited energy; dashed line is the specific energy ( $Q/V[mJ \cdot m^3]$ ).

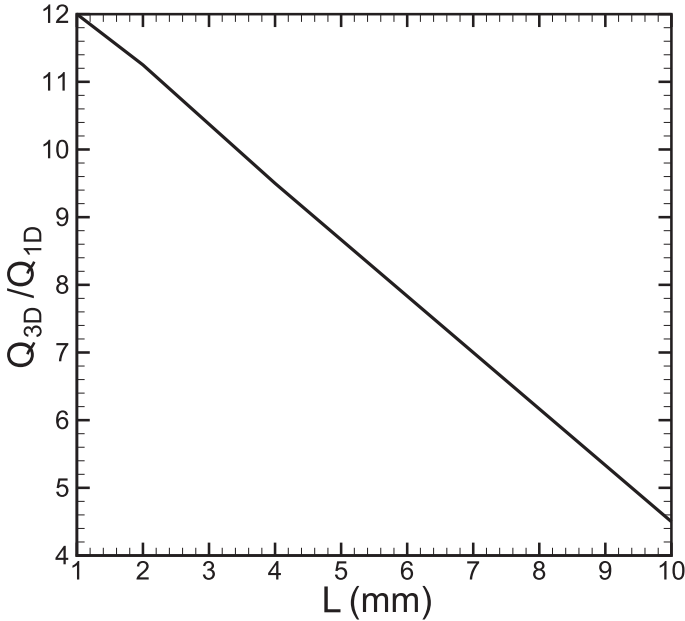


FIG. 14. The ratio of energies required for detonation initiation in  $H_2 - O_2$  obtained for 3D and 1D model versus the size (radius) of the hot spot for  $\Delta t_Q = 1\mu$ .

agrees with the extrapolation of the dependence shown in Fig. 13.

**VI. DISCUSSION AND CONCLUSIONS**

In the present paper we used detailed chemical kinetics and transport models to study consequences of localized

transient energy deposition into a stoichiometric mixture of hydrogen-oxygen leading to the ignition of different regimes of combustion. It is shown that depending on the parameters of energy deposition (deposited energy amount, deposition time scale and size of the hot spot) there are two main mechanisms of reaction wave initiation: the Zeldovich gradient mechanism Ref.<sup>2</sup> and the volumetric thermal explosion (which actually represents one of the asymptotics of the Zeldovich mechanism for the gradient of zero steepness). For practically important time scales the principal scenarios of ignition are: 1) for sub-microsecond pulses the volumetrical explosion takes place inside the hot spot; 2) for microsecond pulses the gradient of temperature and pressure arises on the profile created by the rarefaction wave and ignition starts via Zeldovich mechanism on the gradient of induction time; 3) for millisecond pulses gasdynamical expansion gives rise to a temperature gradient at approximately constant pressure, and the ignition starts according to the Zeldovich mechanism Ref.<sup>2</sup> with all the features inherent to chain-branching chemistry disclosed in Ref.<sup>6</sup>. In the three-dimensional case spherical expansion of the hot spot weakens the generated shock wave in favor of an intensified rarefaction wave. It results in sufficient drop in temperature and pressure in the hot spot on the time scales of the order of acoustic time. Thus, for the same conditions as in one-dimensional case, a less intensive combustion regime arises. The deflagration regimes are less sensitive. However to obtain detonation one should increase sufficiently the power of the energy source. For example for  $L = 1mm$  and  $\Delta t_Q = 1\mu s$  the energy amount is about 10-12 times larger compared to that obtained via extrapolating of the results of 1D model. This is clearly seen from Fig. 14, which shows the ratio of energy required for the detonation initiation in 1D and 3D cases. The calculations were done for the fixed time of the energy deposition  $\Delta t_Q = 1\mu s$ , for the planar and spherical hot spots of different sizes ( $L$  in 1D case and  $R + L$  for 3D case). In particular, it is seen that with the increase of the hot spot size, and corresponding increase of the acoustic time  $t_a$ , the role of a rarefaction wave becomes less important.

**ACKNOWLEDGMENTS**

This research was supported by the Grant of Russian Ministry of Science and Education "Non-stationary combustion regimes for highly efficient and safety energy production" (Program 1.5/XX, Contract No. 8648) and partially supported by the EC FP7 project ERC PBL-PMES (No. 227915). The authors appreciate valuable discussions with V. E. Fortov.

- 
- \* alexeykiverin@gmail.com  
 † misha.liberman@gmail.com
- <sup>1</sup> A.K. Oppenheim and R.I. Soloukhin, *Ann. Rev. Fluid Mechanics*, **5**, 31 (1973).
  - <sup>2</sup> Ya. B. Zeldovich, *Combust. Flame*, **39**, 219 (1980).
  - <sup>3</sup> D. R. Kassoy, *J. Eng. Math.* **68**, 249 (2010).
  - <sup>4</sup> J. F. Clarke, D. R. Kassoy and N. Riley, *Proc. Roy. Soc. Lond.*, **A408**, 129 (1986).
  - <sup>5</sup> T. Echekki, J.H. Chen, *Combust. Flame*, **134**, 169 (2003).
  - <sup>6</sup> M. A. Liberman, A. D. Kiverin, M. F. Ivanov, *Phys. Rev.* **85**, 056312 (2012).
  - <sup>7</sup> J. F. Clarke, D. R. Kassoy and N. Riley, *Proc. Roy. Soc. London*, **A393**, 309 (1984).
  - <sup>8</sup> J. F. Clarke, D. R. Kassoy and N. Riley, *Proc. Roy. Soc. London*, **A393**, 331 (1984).
  - <sup>9</sup> J. F. Clarke, D. R. Kassoy and N. Riley, *Proc. Roy. Soc. Lond.*, **A408**, 129 (1986).
  - <sup>10</sup> J. F. Clarke, D. R. Kassoy, N.E. Maharzi, et al., *Proc. Roy. Soc. Lond.*, **A429**, 259 (1990).
  - <sup>11</sup> A. Sileem, D. R. Kassoy and AK Hayashi, *Proc. Roy. Soc. Lond.* **A435**, 459 (1991).
  - <sup>12</sup> D. R. Kassoy, J. A. Kuehn, M. W. Nability, and J. F. Clarke, *Combust. Theory Model.*, **12**, 1009 (2008).
  - <sup>13</sup> J. D. Regele, D. R. Kassoy, O. V. Vasilyev, *Combust. Theory Model.*, **16**, 650 (2012).
  - <sup>14</sup> T. M. Sloane and P. D. Ronney, *Combust. Sci. and Tech.*, **88**, 1 (1993).
  - <sup>15</sup> J. Warnatz, U. Maas, *Combust. Flame*, **74**, 53 (1988).
  - <sup>16</sup> L. D. Landau and E. M. Lifshitz, *Fluid Mechanics*, Pergamon Press, Oxford, 1989.
  - <sup>17</sup> J. Warnatz, U. Maas, R. W. Dibble, *Combustion. Physical and chemical fundamentals, modeling and simulations, experiments, pollutant formation*, Springer, 2001.
  - <sup>18</sup> J. B. Heywood, *Internal combustion engine fundamentals*, Mc.Graw-Hill, New York. 1988.
  - <sup>19</sup> J. O. Hirschfelder, C. F. Gurtiss, R. B. Bird, *Molecular theory of gases and liquids*, Wiley, New York, 1964.
  - <sup>20</sup> O.M. Belotserkovsky, Yu.M. Davydov, *Coarse-particle method in hydrodynamics* (Russian Publ. Inc. Nauka, Mir), Moscow, 1982.
  - <sup>21</sup> M. F. Ivanov, A. D. Kiverin, M. A. Liberman, *Phys. Rev.* **E 83**, 056313: 1-16 (2011).
  - <sup>22</sup> M. F. Ivanov, A. D. Kiverin, M. A. Liberman, *Int. J. Hydrogen Energy*, **36**, 7714 (2011).
  - <sup>23</sup> M.A. Liberman, M.F. Ivanov, D.M. Valiev, *Combust. Sci. Tech.*, **178**, 1613 (2006).
  - <sup>24</sup> M.A. Liberman, M.F. Ivanov, O.D. Peil, D.M. Valiev, *Combust. Sci. Tech.*, **177**, 151 (2005).
  - <sup>25</sup> Ya. B. Zeldovich and Yu. P. Raizer, *Physics of Shock waves and High-Temperature Hydrodynamic Phenomena*, Academic Press, New-York-London 1966.
  - <sup>26</sup> P. Reinicke and J. Meyer-ter-Vehn, *The point explosion with heat conduction*, *Phys. Fluids* **A3 7**, 1807 (1991).
  - <sup>27</sup> D. Lewis and G. von Elbe, *Combustion, Flames and Explosion of Gases*, 2nd ed. Part 1, Academic Press, New York, 1961.